

Scientific paper

The (p, ρ, T) Properties and Apparent Molar Volumes V_ϕ of $\text{LiNO}_3 + \text{C}_2\text{H}_5\text{OH}$

Huseyn Israfilov,¹ Rasim Jannataliyev,^{1,2} Javid Safarov,^{1,2*}
Astan Shahverdiyev¹ and Egon Hassel²

¹ Department "Heat and Refrigeration Techniques", Azerbaijan Technical University,
H. Javid Avn. 25, AZ1073 Baku, Azerbaijan.

² Lehrstuhl für Technische Thermodynamik, Universität Rostock, 18059, Rostock, Germany.

* Corresponding author: E-mail: javid.safarov@uni-rostock.de
Phone: + 49 381 4989415; fax: + 49 381 4989402

Received: 15-10-2008

Dedicated to Professor Josef Barthel on the occasion of his 80th birthday

Abstract

The (p, ρ, T) properties and apparent molar volumes V_ϕ of LiNO_3 in ethanol at temperatures $T = (298.15 \text{ to } 398.15) \text{ K}$ and pressures up to $p = 40 \text{ MPa}$ are reported. The vibration tube densimeter method used during the experiments. The experiments were carried out at molalities of $m = (0.12071, 0.26234, 0.60237, 0.97956, 1.83765, 2.62045 \text{ and } 3.27773) \text{ mol kg}^{-1}$ using lithium nitrate. An empirical correlation for the density of $(\text{LiNO}_3 + \text{C}_2\text{H}_5\text{OH})$ with pressure, temperature and molality has been derived. The short form of equation of state was developed for the technical calculations. Apparent molar volume and thermal properties of LiNO_3 in ethanol were calculated using the equation of state.

Keywords: Apparent molar volume, density, partial molar volume, vibration tube densimeter, isothermal compressibility, isobaric thermal expansibility, lithium nitrate

1. Introduction

In absorption heat pump systems, compression of the heat transfer fluid is achieved thermally in a solution circuit which consists of an absorber, a solution pump, a generator and an expansion valve. Vapour of refrigerant with low pressure from the evaporator is absorbed in the absorbent and this process generates heat. The solution is pumped to high pressure and then enters the generator, where the heat transfer fluid is boiled off with an external heat supply at a high temperature. The vapour of refrigerant is condensed in the condenser while the absorbent is returned to the absorber via the expansion valve. Heat is extracted from the heat source in the evaporator. Useful heat is given off at medium temperature in the condenser and in the absorber. In the generator high-temperature heat is supplied to run the process. A small amount of electricity may be needed to operate the solution pump.

The efficiency of an absorption heat transfer cycle largely depends on the physical and chemical properties

of the heat transfer fluid. The problems of using conventional aqueous solutions of electrolytes were discussed in our previous publications on methanol and ethanol solutions of electrolytes.^{1–3} Total analysis of the thermodynamic properties of non-aqueous electrolyte solutions were carried out by Prof. Barthel and his research group.^{4–6}

This work is a continuation of the study of solutions of electrolytes for their future application as heat transfer fluids in absorption systems. These systems (alcohol solutions of electrolyte) could replace aqueous solutions at temperatures below the freezing point of water. Ethanol has a freezing temperature lower than methanol and can improve the circulation of heat transfer agents in the closed system.

The (p, ρ, T) properties and apparent molar volumes V_ϕ of the LiNO_3 in ethanol at $T = (298.15 \text{ to } 398.15) \text{ K}$ and pressures up to $p = 40 \text{ MPa}$ are reported. An empirical correlation for the density of $(\text{LiNO}_3 + \text{C}_2\text{H}_5\text{OH})$ with pressure, temperature and molality has been derived.

Various literature works^{7–10} with thermodynamic properties of LiNO_3 in ethanol are available. Glugla *etc.*⁷ investigated the partial molar volume of monovalent salts and polar molecules in organic solvents. High volume injection and flow dilatometers were used during the experiments. The temperature bath used with this apparatus controlled temperature fluctuation to within 0.001 °C. The volume change was always less than 0.0001 ml and frequently less than 0.00005 ml. The apparent molar volumes of LiNO_3 in ethanol were measured at temperature $T = 298.15$ K, molalities $m = (0.00201 \text{ to } 2.4085) \text{ mol kg}^{-1}$ and at $p = 0.1$ MPa. The partial molar volumes measured in aprotic solvents with this apparatus were accurate to better than ± 2 %.

Eliseeva *etc.*⁸ in 1999, investigated the density of $\text{LiNO}_3 + \text{ethanol}$ at $T = 298.15$ K and at molalities $m = (0.1048 \text{ to } 3.0026) \text{ mol kg}^{-1}$ using a well known vibration-tube densimeter method. The uncertainties of measurements of this work is $2 \times 10^{-6} \text{ g cm}^{-3}$.

Marcus and Hefter,¹⁰ in 2004, after the analysis of available literature results decided the apparent molar volume at infinite dilution, as $V_\phi^0 = -5 \text{ cm}^3 \text{ mol}^{-1}$ at $T = 298.15$ K.

Verevkin *et al.*, in 2006, measured the vapor pressure p of $(\text{LiNO}_3 + \text{C}_2\text{H}_5\text{OH})$ solutions at $T = (298.15 \text{ to } 323.15) \text{ K}$. The experiments were carried out in the molality range $m = (0.19125 \text{ to } 2.21552) \text{ mol kg}^{-1}$. The Antoine equation was used for the empirical description of the experimental vapor pressure results, and the Pitzer-

Mayorga model with inclusion of Archer's ionic strength dependence of the third virial coefficient for the calculated osmotic coefficients were used for the evaluation of the osmotic, activity coefficients (ϕ , γ) and activity of solvent a_s from the experimental vapor pressure results.

The (p, ρ, T) properties of these solutions are not available in the literature.

2. Experimental Section

The (p, ρ, T) measurements were studied using a new modernized high pressure – high temperature vibrating tube densimeter DMA HPM (Anton-Paar, Austria). The schematic principle of the vibration tube densimeter is shown in Figure 1. The measurements with a vibrating tube are based on the dependence between the period of oscillation of a unilaterally fixed U-tube Hastelloy C-276 and its mass. This mass consists of the U-tube material and the mass of the fluid filled into the U-tube. The behavior of the vibrating tube can be described by the simple mathematical-physical model of the undamped spring-mass system.¹¹ The characteristic period of oscillation τ (μs) of this model is described by the following equation:

$$\tau = 2\pi \sqrt{\frac{m_0 + V\rho}{k}}, \quad (1)$$

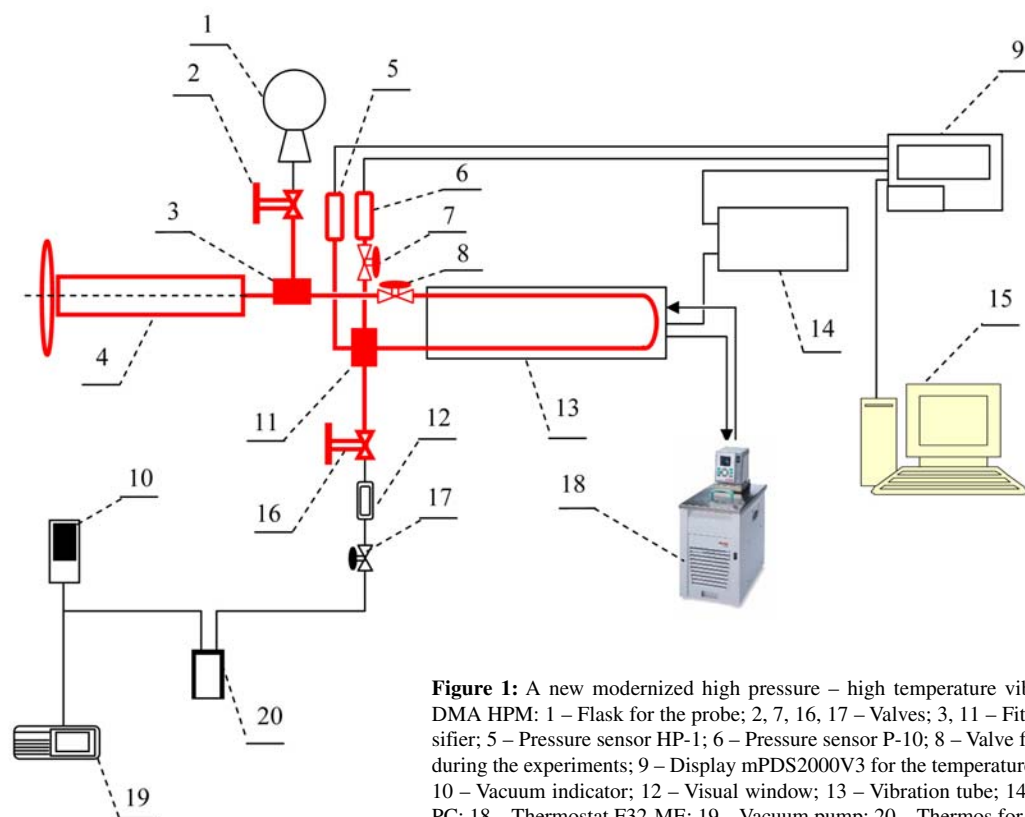


Figure 1: A new modernized high pressure – high temperature vibrating tube densimeter DMA HPM: 1 – Flask for the probe; 2, 7, 16, 17 – Valves; 3, 11 – Fitting; 4 – Pressure intensifier; 5 – Pressure sensor HP-1; 6 – Pressure sensor P-10; 8 – Valve for the closing of system during the experiments; 9 – Display mPDS2000V3 for the temperature and frequency control; 10 – Vacuum indicator; 12 – Visual window; 13 – Vibration tube; 14 – Interface mode; 15 – PC; 18 – Thermostat F32-ME; 19 – Vacuum pump; 20 – Thermos for cooling.

where: τ is the period of oscillation of the vibration tube, μs ; m_0 is mass of the empty vibrating tube, kg ; V is volume of the vibrating tube, m^3 ; ρ is sample density, kg m^{-3} and k is the spring constant, N m^{-1} .

The period of oscillation measurement and the temperature control is implemented within the DMA HPM control system, which consists of a measuring cell (13) and a modified mPDS2000V3 control unit (9) connected to a PC (15) via an interface (14). The temperature in the measuring cell was controlled using a thermostat (18) F32-ME (Julabo, Germany) with an error of ± 10 mK and was measured using the (ITS-90) Pt100 thermometer with an experimental error of ± 15 mK. Pressure was created by a pressure intensifier (4) (Type 37-6-30, HIP, USA) and measured by pressure transmitter (6) (P-10, WIKA Alexander Wiegand GmbH & Co., Germany) with a measuring error of 0.1%. The observed reproducibility and estimated maximum uncertainty of the density measurements at temperatures $T = (298.15 \text{ to } 398.15)$ K and at pressures up to $p = 40$ MPa is within $\pm 0.1\text{--}0.3$ kg m^{-3} . All high pressure valves (2, 7, 8, 16, 17), tubes, fittings (3 and 11) etc. were supplied by SITEC and NOVA (Switzerland).

Rearrangement of the equation and substitution of the mechanical constants lead to the classical equation for vibrating tube densimeters:

$$\rho = A - B\tau^2, \quad (2)$$

where: ρ is the sample density, kg m^{-3} and τ is the period of oscillation, μs . The parameters A and B were determined by substance calibration measuring the period of oscillation of at least two samples with known density. Water¹² (twice-distilled), ethanol^{13–15} and NaCl (aq)^{16–17} in various molalities were used as reference substances for the calibration of the installation.

Unfortunately, the parameters A and B are highly temperature and also pressure dependent. Therefore, the parameters must be determined for each temperature and pressure separately or, like in this work, the classical equation must be expanded with temperature and pressure-dependent terms. For measurements at $T = (298.15 \text{ to } 398.15)$ K and up to $p = 40$ MPa an extended calibration equation with 14 significant parameters is employed:¹⁸

$$A = \sum_i a_i (T / \text{K})^i + \sum_j b_j (p / \text{MPa})^j + c(T / \text{K})(p / \text{MPa}), \quad (3)$$

$$B = \sum_i d_i (T / \text{K})^i + \sum_j e_j (p / \text{MPa})^j + f(T / \text{K})(p / \text{MPa}), \quad (4)$$

where: $a_0, a_1, a_2, a_3, b_1, b_2, c, d_0, d_1, d_2, d_3, e_1, e_2$ and f are the parameters of the these extended vibrating tube equations.

Before starting the experiment only the valve of the flask (1) was closed. The sample filled into the measuring cell was under vacuum, which is connected to the installation. Vacuum is applied over (3 to 4) hours using a vacuum pump (19) (Model S 1.5, Leybold, Germany) until a minimal pressure [(3 to 5) Pa] has been reached (measured with digital vacuum indicator (10) THERMOVAC TM 100 (Leybold, Germany)). The valve (17) is closed and the valve of the flask is opened. The investigated substance is filled into the measuring system. For the tracing of flow of the measured sample a special window (12) was constructed between valves (16) and (17). After filling of the system, the valves (2) and (16), which separate the high pressure connections (bold lines in Fig.1) from others, were closed. The experiments were started usually at low pressures in the measured cell (0.8–1.0 MPa). Temperature stabilization was around two hours. The period of oscillation of the vibration tube is taken from the display of the mPDS2000V3 control system (9).

To check the apparatus and procedures of the measurements and the accuracy of calibration before engaging in measurements on solutions, the density of double distilled water, ethanol and NaCl (aq) with various molalities were measured, compared with the values of literature results and good comparison were obtained.

LiNO_3 ($w > 0.998$) was supplied from Merck, Germany and was used without further purification. Before experiment it was dried about 48 h in a special cell by heating at 413.15 K and reduced pressure (around 7–8 Pa).

Ethanol ($w > 0.998$) was supplied from Merck, Germany and was degassed by vacuum distillation using a Vigreux column with a height of 90 cm. The final purity of the ethanol was checked by gas chromatography ($w > 0.999$) and Karl-Fischer titration (water content <50 ppm).

For the preparation of samples, flasks with LiNO_3 and ethanol were connected to the vacuum pump using a glass adapter. Before the opening of valves of flasks air in the glass adapter was evacuated. Ethanol, in the top flask, flew to the down flask, where was LiNO_3 under vacuum. The samples were obtained by successive dilutions of the concentrated solutions. The solutions were prepared by mass using an electronic scale ED224S (Sartorius, Germany) with a resolution of 0.0001 g.

3. Results and Discussion

The (p, ρ, T) properties and apparent molar volumes V_ϕ of ($\text{LiNO}_3 + \text{C}_2\text{H}_5\text{OH}$) were studied at $T = (298.15 \text{ to } 398.15)$ K, pressures up to $p = 40$ MPa and molalities $m = (0.12071, 0.26234, 0.60237, 0.97956, 1.83765, 2.62045, \text{ and } 3.27773)$ mol kg^{-1} of lithium nitrate. Experiments were carried out in the $T = 25$ K and $p = 5$ MPa intervals. The experimental (p, ρ, T) results are listed in Table 1.

Table 1. Experimental values of pressure p/MPa , density $\rho/\text{kg m}^{-3}$, temperature T/K , isothermal compressibility $kT \cdot 10^6/\text{MPa}^{-1}$, isobaric thermal expansivity $\alpha_p \cdot 10^6/\text{K}^{-1}$, difference in isobaric and isochoric heat capacities $(c_p - c_v)/(\text{Jkg}^{-1}\text{K}^{-1})$ of the $(\text{LiNO}_3 + \text{C}_2\text{H}_5\text{OH})$.

p/MPa	ρ $/\text{kg m}^{-3}$	T/K	$k_T \cdot 10^6$ $/\text{MPa}^{-1}$	$\alpha_p \cdot 10^6/\text{K}^{-1}$	$(c_p - c_v)$ $/\text{Jkg}^{-1}\text{K}^{-1}$	p/MPa	ρ $/\text{kg m}^{-3}$	T/K	$k_T \cdot 10^6$ $/\text{MPa}^{-1}$	$\alpha_p \cdot 10^6/\text{K}^{-1}$	$(c_p - c_v)$ $/\text{Jkg}^{-1}\text{K}^{-1}$
$m = 0.12071 \text{ mol} \cdot \text{kg}^{-1}$											
0.214	791.56	298.15	1145.1	1086.9	388.5	0.324	775.93	323.15	1338.9	1172.7	427.7
5.012	795.70	298.15	1077.7	1051.5	384.4	5.004	780.50	323.15	1251.6	1128.8	421.5
10.023	799.81	298.15	1015.3	1018.4	380.8	10.006	785.22	323.15	1168.6	1086.4	415.7
15.412	804.05	298.15	955.5	986.1	377.4	15.745	790.30	323.15	1086.4	1043.8	410.1
20.026	807.53	298.15	909.4	961.0	374.9	19.998	793.91	323.15	1032.1	1015.3	406.5
25.621	811.56	298.15	859.3	933.3	372.4	25.006	797.95	323.15	975.2	984.9	402.8
30.012	814.59	298.15	823.8	913.3	370.6	29.992	801.77	323.15	924.7	957.6	399.7
35.032	817.89	298.15	787.0	892.5	368.9	35.004	805.39	323.15	879.6	933.0	397.1
39.984	821.00	298.15	754.1	873.6	367.5	39.998	808.79	323.15	839.6	910.8	394.8
0.321	769.50	323.15	1377.0	1181.7	425.9	0.326	752.51	348.15	1637.4	1298.5	476.4
5.412	774.59	323.15	1277.2	1132.0	418.5	5.006	757.87	348.15	1511.7	1239.7	467.0
9.989	778.98	323.15	1198.1	1091.9	412.8	9.997	763.39	348.15	1394.0	1183.8	458.5
15.014	783.52	323.15	1122.3	1052.9	407.4	15.006	768.48	348.15	1295.1	1136.0	451.5
20.002	787.76	323.15	1056.6	1018.7	402.9	19.998	773.36	348.15	1207.9	1093.3	445.5
25.001	791.87	323.15	997.2	987.3	398.9	25.008	777.91	348.15	1132.9	1056.0	440.5
29.996	795.77	323.15	944.4	959.0	395.4	29.998	782.19	348.15	1067.2	1022.9	436.4
35.478	799.80	323.15	893.3	931.2	392.2	35.004	786.26	348.15	1008.8	993.1	432.9
39.989	802.93	323.15	855.8	910.6	389.9	39.998	790.09	348.15	957.2	966.4	429.9
0.245	745.71	348.15	1697.4	1330.3	486.7	0.385	727.08	373.15	2057.1	1480.9	547.2
5.025	751.36	348.15	1559.9	1265.8	475.9	5.009	733.49	373.15	1866.4	1397.5	532.3
10.003	756.89	348.15	1438.0	1207.7	466.5	10.213	740.23	373.15	1688.3	1318.1	518.7
15.301	762.47	348.15	1326.3	1153.5	458.1	15.008	745.94	373.15	1553.1	1256.8	508.8
19.998	767.14	348.15	1240.7	1111.3	451.8	19.998	751.60	373.15	1431.5	1200.8	500.1
25.065	771.82	348.15	1161.3	1071.7	446.1	25.318	757.10	373.15	1323.9	1150.5	492.8
29.997	776.15	348.15	1093.2	1037.1	441.4	29.994	761.66	373.15	1241.9	1111.6	487.5
35.001	780.37	348.15	1031.2	1005.3	437.2	35.006	766.25	373.15	1165.2	1074.8	482.8
39.998	784.29	348.15	977.3	977.2	433.8	39.994	770.59	373.15	1097.7	1041.9	478.9
0.365	719.91	373.15	2145.2	1535.1	569.4	0.748	699.11	398.15	2675.9	1751.0	652.5
5.142	726.71	373.15	1934.3	1442.4	552.3	5.004	706.37	398.15	2390.4	1632.7	628.6
10.003	733.03	373.15	1760.2	1364.5	538.4	10.009	714.29	398.15	2119.5	1518.3	606.3
15.621	739.89	373.15	1592.0	1287.8	525.4	15.621	722.22	398.15	1884.1	1416.9	587.4
19.998	744.90	373.15	1481.1	1236.4	517.0	19.998	728.01	398.15	1731.6	1350.0	575.6
25.004	750.33	373.15	1371.0	1184.6	509.1	25.026	734.12	398.15	1586.1	1285.2	564.8
29.996	755.36	373.15	1277.5	1140.0	502.5	29.996	739.79	398.15	1463.7	1229.9	556.2
35.030	760.16	373.15	1195.1	1100.1	497.1	35.007	745.05	398.15	1359.8	1182.3	549.3
39.997	764.57	373.15	1124.8	1065.6	492.7	39.992	749.99	398.15	1270.0	1140.5	543.7
$m = 0.26234 \text{ mol} \cdot \text{kg}^{-1}$						$m = 0.60237 \text{ mol} \cdot \text{kg}^{-1}$					
0.894	691.62	398.15	2798.2	1819.5	681.1	0.362	813.11	298.15	1055.1	1078.2	404.0
5.004	698.72	398.15	2505.0	1698.4	656.2	5.006	817.04	298.15	996.2	1045.2	400.2
10.006	706.73	398.15	2217.3	1577.4	632.2	10.008	820.95	298.15	941.4	1014.0	396.7
15.201	714.38	398.15	1978.6	1474.9	612.8	14.995	824.76	298.15	891.5	985.2	393.6
20.003	720.88	398.15	1799.3	1396.5	598.7	19.998	828.39	298.15	846.8	959.0	390.9
25.621	727.87	398.15	1627.4	1320.0	585.7	25.006	831.79	298.15	807.3	935.5	388.5
29.998	732.97	398.15	1513.9	1268.8	577.6	29.994	835.10	298.15	770.9	913.5	386.5
35.002	738.49	398.15	1401.4	1217.2	570.0	35.004	838.27	298.15	737.8	893.3	384.7
39.996	743.49	398.15	1307.7	1173.6	564.1	39.998	841.29	298.15	707.8	874.7	383.1
0.215	798.01	298.15	1115.8	1089.6	397.6	0.415	790.94	323.15	1260.0	1143.8	424.2
5.001	802.13	298.15	1050.5	1054.3	393.3	5.009	795.34	323.15	1181.3	1104.3	419.4
10.003	806.18	298.15	990.6	1021.5	389.5	10.621	800.49	323.15	1096.5	1061.0	414.4
15.210	810.22	298.15	935.0	990.5	386.1	15.048	804.32	323.15	1038.0	1030.7	411.2
19.998	813.79	298.15	888.8	964.4	383.4	19.998	808.37	323.15	980.2	1000.3	408.1
25.006	817.36	298.15	845.3	939.5	380.9	25.005	812.27	323.15	928.0	972.6	405.5
29.996	820.76	298.15	806.2	916.8	378.8	29.997	815.94	323.15	881.9	947.7	403.3
35.006	824.01	298.15	770.8	896.1	376.9	35.006	819.40	323.15	840.9	925.2	401.5
39.997	827.09	298.15	738.9	877.1	375.3	39.998	822.62	323.15	804.7	905.2	400.0
						0.514	768.00	348.15	1521.4	1235.1	454.6

p/MPa	ρ $/\text{kg m}^{-3}$	T/K	$k_T \cdot 10^6$ $/\text{MPa}^{-1}$	$\alpha_p \cdot 10^6/\text{K}^{-1}$ K^{-1}	$(c_p - c_v)$ $/\text{Jkg}^{-1}\text{K}^{-1}$	p/MPa	ρ $/\text{kg m}^{-3}$	T/K	$k_T \cdot 10^6$ $/\text{MPa}^{-1}$	$\alpha_p \cdot 10^6/\text{K}^{-1}$ K^{-1}	$(c_p - c_v)$ $/\text{Jkg}^{-1}\text{K}^{-1}$
5.002	773.02	348.15	1412.3	1184.6	447.5	19.998	782.75	373.15	1254.9	1083.8	446.2
10.006	778.36	348.15	1306.3	1134.8	440.9	25.003	787.47	373.15	1173.6	1045.5	441.3
15.024	783.32	348.15	1216.2	1091.8	435.6	29.941	791.86	373.15	1103.5	1012.0	437.4
20.032	788.04	348.15	1137.2	1053.6	431.2	35.006	796.00	373.15	1041.8	982.3	434.2
25.034	792.36	348.15	1070.2	1020.7	427.8	39.998	799.93	373.15	986.9	955.6	431.6
29.998	796.46	348.15	1010.8	991.2	424.9	0.741	734.42	398.15	2226.0	1538.5	576.5
35.005	800.32	348.15	958.3	964.8	422.6	5.003	741.10	398.15	2008.6	1440.8	555.2
39.986	803.93	348.15	912.1	941.3	420.7	10.214	748.59	398.15	1794.2	1342.8	534.5
0.324	743.06	373.15	1896.3	1386.6	509.2	15.026	754.86	398.15	1635.3	1269.0	519.4
5.102	749.52	373.15	1720.1	1309.3	496.2	19.996	760.76	398.15	1500.7	1205.6	506.9
10.068	755.71	373.15	1569.3	1242.0	485.4	25.004	766.31	398.15	1385.8	1150.8	496.5
15.027	761.42	373.15	1443.9	1185.2	476.8	29.996	771.35	398.15	1290.1	1104.6	488.1
20.129	766.91	373.15	1334.4	1134.9	469.6	35.002	776.12	398.15	1206.6	1063.7	481.1
25.046	771.77	373.15	1245.5	1093.4	464.1	39.992	780.47	398.15	1135.8	1028.8	475.4
29.998	776.33	373.15	1168.3	1057.0	459.6	$m = 1.83765 \text{ mol} \cdot \text{kg}^{-1}$					
35.106	780.70	373.15	1099.5	1024.1	455.9	0.214	862.26	298.15	910.6	983.6	367.4
39.997	784.73	373.15	1040.2	995.5	453.0	5.002	866.01	298.15	862.0	957.8	366.4
0.624	716.11	398.15	2442.2	1634.3	608.1	10.064	869.65	298.15	817.7	933.9	365.7
4.997	723.29	398.15	2185.5	1524.8	585.6	15.023	873.15	298.15	777.6	911.8	365.1
10.008	730.89	398.15	1948.2	1421.8	565.2	20.004	876.42	298.15	742.3	891.9	364.6
15.406	738.28	398.15	1746.2	1332.4	548.2	25.006	879.59	298.15	709.8	873.3	364.2
20.007	744.09	398.15	1604.6	1268.7	536.7	30.002	882.65	298.15	680.0	856.0	364.0
25.106	749.95	398.15	1475.2	1209.6	526.6	35.014	885.64	298.15	652.3	839.6	363.8
29.996	755.18	398.15	1369.8	1160.8	518.6	39.998	888.41	298.15	627.8	824.9	363.7
35.008	760.14	398.15	1277.9	1117.7	512.1	0.214	840.77	323.15	1061.2	1030.4	384.6
39.994	764.73	398.15	1199.1	1080.4	506.8	5.007	844.96	323.15	998.4	1000.3	383.2
$m = 0.97956 \text{ mol} \cdot \text{kg}^{-1}$						10.068	849.17	323.15	939.8	971.6	382.2
0.231	829.01	298.15	1002.9	1051.8	396.7	15.924	853.78	323.15	880.2	941.9	381.5
5.512	833.15	298.15	944.0	1018.9	393.6	19.996	856.81	323.15	843.4	923.3	381.2
10.132	836.69	298.15	896.9	992.2	391.1	25.007	860.35	323.15	802.7	902.4	381.1
14.905	840.24	298.15	852.4	966.5	388.8	29.962	863.64	323.15	766.9	883.8	381.1
19.821	843.65	298.15	812.1	942.8	386.8	35.007	866.77	323.15	734.6	866.8	381.3
25.133	847.19	298.15	772.6	919.3	384.9	39.996	869.86	323.15	704.2	850.6	381.7
30.621	850.70	298.15	735.6	896.8	383.2	0.524	818.88	348.15	1249.9	1086.3	401.4
35.004	853.42	298.15	708.4	880.1	382.0	5.008	823.67	348.15	1165.3	1046.8	397.4
39.987	856.31	298.15	680.8	862.8	380.8	10.009	828.39	348.15	1088.5	1010.4	394.2
0.301	806.79	323.15	1190.9	1108.5	413.3	15.712	833.51	348.15	1011.8	973.5	391.2
5.061	811.29	323.15	1115.0	1071.2	409.9	20.005	837.03	348.15	962.8	949.6	389.6
10.245	815.95	323.15	1042.5	1035.0	406.9	25.601	841.38	348.15	906.0	921.6	388.0
15.329	820.13	323.15	982.1	1004.3	404.6	29.993	844.60	348.15	866.4	901.9	387.0
20.214	824.02	323.15	929.6	977.2	402.9	35.004	848.15	348.15	825.1	881.1	386.2
25.024	827.63	323.15	883.8	953.3	401.5	39.996	851.44	348.15	788.9	862.7	385.7
30.005	831.15	323.15	841.7	931.0	400.4	0.921	797.03	373.15	1492.2	1177.3	434.9
35.214	834.59	323.15	802.8	910.1	399.5	5.007	801.74	373.15	1391.5	1129.5	426.7
39.998	837.64	323.15	770.0	892.3	398.9	10.006	807.19	373.15	1284.8	1078.3	418.4
0.301	783.98	348.15	1427.2	1181.9	434.7	15.621	812.90	373.15	1183.3	1028.9	410.7
5.023	789.22	348.15	1320.9	1133.3	428.9	19.997	817.05	373.15	1115.4	995.5	405.7
10.004	794.29	348.15	1226.9	1089.6	424.1	25.412	821.76	373.15	1043.7	959.8	400.8
15.302	799.38	348.15	1140.4	1048.8	420.1	29.998	825.56	373.15	989.8	932.7	397.2
19.994	803.61	348.15	1074.0	1017.1	417.3	35.006	829.31	373.15	939.8	907.3	394.1
25.323	808.01	348.15	1009.6	985.9	414.8	39.997	832.98	373.15	893.6	883.6	391.4
29.954	811.67	348.15	959.5	961.4	413.2	1.024	772.35	398.15	1891.3	1364.8	507.7
35.064	815.51	348.15	910.0	936.9	411.8	5.006	777.99	398.15	1736.4	1289.0	489.7
39.995	818.94	348.15	868.3	916.0	410.8	10.331	785.04	398.15	1563.4	1203.2	469.7
0.365	760.19	373.15	1748.3	1308.3	480.6	15.006	790.63	398.15	1440.5	1141.5	455.5
5.004	766.10	373.15	1599.6	1241.9	469.6	19.985	796.07	398.15	1331.6	1086.1	443.1
10.326	772.49	373.15	1455.5	1176.6	459.4	25.004	801.25	398.15	1236.8	1037.4	432.4
15.032	777.69	373.15	1349.4	1127.8	452.3	29.996	805.94	398.15	1157.6	996.2	423.5

p/MPa	ρ /kg · m ⁻³	T/K	$k_T \cdot 10^6$ /MPa ⁻¹	$\alpha_p \cdot 10^6/\text{K}^{-1}$ K ⁻¹	$(c_p - c_v)$ /Jkg ⁻¹ K ⁻¹
35.004	810.31	398.15	1089.1	960.2	416.0
39.998	814.43	398.15	1028.7	928.3	409.5
$m = 2.62045 \text{ mol} \cdot \text{kg}^{-1}$					
0.542	890.14	298.15	823.8	913.6	339.4
4.963	893.17	298.15	789.6	896.2	339.5
9.891	896.55	298.15	753.4	877.6	339.9
15.104	899.98	298.15	718.7	859.6	340.6
19.839	902.87	298.15	690.8	845.1	341.4
25.099	906.26	298.15	659.8	828.9	342.5
29.769	908.94	298.15	636.4	816.5	343.6
35.058	912.04	298.15	610.6	802.8	345.1
39.930	914.74	298.15	589.1	791.3	346.5
1.071	869.76	323.15	949.1	960.9	361.4
4.856	872.84	323.15	908.5	939.0	359.3
9.907	876.78	323.15	859.6	912.4	357.0
15.102	880.58	323.15	815.3	888.1	355.0
19.702	883.86	323.15	779.2	868.1	353.6
25.163	887.55	323.15	740.8	846.6	352.3
29.746	890.53	323.15	711.4	830.0	351.4
35.061	893.73	323.15	681.3	812.8	350.6
39.882	896.67	323.15	655.0	797.7	350.1
1.054	848.34	348.15	1126.8	1024.6	382.4
4.986	852.06	348.15	1068.4	993.6	377.5
10.025	856.65	348.15	1001.3	957.4	372.0
15.625	861.30	348.15	938.3	922.9	366.9
20.036	864.85	348.15	893.3	897.9	363.3
25.415	868.92	348.15	844.8	870.7	359.5
29.985	872.21	348.15	807.9	849.7	356.7
35.026	875.68	348.15	770.9	828.4	353.9
39.986	878.86	348.15	738.7	809.7	351.5
1.816	827.11	373.15	1346.4	1093.8	400.9
5.020	830.51	373.15	1282.5	1061.5	394.8
9.791	835.54	373.15	1194.4	1016.4	386.3
15.113	840.66	373.15	1112.0	973.4	378.2
19.593	844.80	373.15	1050.3	940.5	372.0
25.103	849.57	373.15	984.0	904.8	365.4
29.987	853.59	373.15	931.9	876.2	360.1
35.029	857.43	373.15	885.2	850.1	355.3
39.927	861.06	373.15	843.4	826.4	350.9
1.945	803.94	398.15	1661.0	1189.2	421.6
4.989	807.76	398.15	1572.9	1148.2	413.2
10.021	814.03	398.15	1440.1	1085.3	400.1
15.024	819.75	398.15	1330.4	1032.1	388.9
20.036	825.07	398.15	1237.0	985.9	379.1
25.412	830.44	398.15	1150.5	942.0	369.8
29.984	834.81	398.15	1085.3	908.3	362.6
35.024	839.23	398.15	1023.7	875.9	355.5
39.987	843.41	398.15	969.1	846.6	349.1
$m = 3.27773 \text{ mol} \cdot \text{kg}^{-1}$					
0.788	911.05	298.15	772.5	843.9	301.7
4.975	913.85	298.15	746.3	833.1	303.4
9.774	916.98	298.15	718.2	822.0	305.9
15.102	920.38	298.15	689.2	811.0	309.1
19.854	923.33	298.15	665.1	802.3	312.5
25.104	926.52	298.15	640.2	793.8	316.7
29.832	929.31	298.15	619.3	787.0	320.9
35.093	932.34	298.15	597.5	780.4	326.0
39.824	934.99	298.15	579.2	775.2	330.9

p/MPa	ρ /kg · m ⁻³	T/K	$k_T \cdot 10^6$ /MPa ⁻¹	$\alpha_p \cdot 10^6/\text{K}^{-1}$ K ⁻¹	$(c_p - c_v)$ /Jkg ⁻¹ K ⁻¹
0.850	891.23	323.15	883.5	916.1	344.4
5.021	894.40	323.15	846.9	892.7	340.0
9.698	897.85	323.15	809.1	868.5	335.5
15.104	901.68	323.15	769.4	843.2	331.2
19.771	904.86	323.15	738.3	823.3	327.9
24.899	908.23	323.15	706.8	803.4	324.9
29.763	911.28	323.15	679.7	786.2	322.5
35.007	914.43	323.15	653.0	769.3	320.3
39.933	917.36	323.15	629.2	754.3	318.5
1.200	870.24	348.15	1068.0	1003.9	377.5
4.955	873.68	348.15	1019.2	971.8	369.2
9.872	878.09	348.15	960.5	932.5	359.0
14.930	882.24	348.15	908.9	897.5	349.7
19.941	886.13	348.15	863.4	866.2	341.4
24.957	889.88	348.15	822.1	837.3	333.6
29.862	893.39	348.15	785.5	811.4	326.6
35.103	897.01	348.15	749.8	785.7	319.5
39.839	900.14	348.15	720.4	764.3	313.6
1.356	848.46	373.15	1306.7	1068.4	384.2
5.024	852.32	373.15	1241.9	1032.1	375.5
9.873	857.18	373.15	1165.8	988.1	364.6
14.922	862.01	373.15	1095.6	946.2	353.7
19.904	866.53	373.15	1034.5	908.4	343.5
25.102	871.05	373.15	977.3	871.9	333.2
29.841	875.06	373.15	929.7	840.6	324.1
35.104	879.19	373.15	883.4	809.2	314.6
40.019	882.94	373.15	843.8	781.5	305.9
1.254	825.83	398.15	1569.0	1078.9	357.7
4.914	830.12	398.15	1488.8	1046.8	353.1
9.756	835.75	398.15	1391.1	1005.5	346.3
14.924	841.55	398.15	1298.5	963.8	338.5
19.922	846.85	398.15	1220.5	926.4	330.6
24.985	851.92	398.15	1151.2	891.0	322.3
29.758	856.52	398.15	1092.4	859.3	314.2
35.103	861.57	398.15	1032.0	824.8	304.6
39.960	865.87	398.15	983.8	795.7	295.9

Using a program for standard thermodynamic analysis to describe the (p, ρ, T) properties of ethanol solutions of LiNO_3 , the equation of state from Ref.¹⁹ was used:

$$p = A\rho^2 + B\rho^8 + C\rho^{12}, \quad (5)$$

where: the coefficients of eqn. (5) A , B and C are functions of temperature and molalities m .

$$A = \sum_{i=1}^4 T^i \sum_{j=0}^3 a_{ij} m^j, \quad (6)$$

$$B = \sum_{i=0}^3 T^i \sum_{j=0}^3 b_{ij} m^j, \quad (7)$$

$$C = \sum_{i=0}^3 T^i \sum_{j=0}^3 c_{ij} m^j. \quad (8)$$

Table 2: Values of the coefficients a_{ij} , b_{ij} and c_{ij} in Eqs. 5–8.

a_{ij}	b_{ij}	c_{ij}
$a_{10} = -3.21735$	$b_{00} = 369.943$	$c_{00} = -5740.52$
$a_{11} = -2.57045$	$b_{01} = -4315.07$	$c_{01} = 17747.3$
$a_{12} = 4.47684$	$b_{02} = 598.959$	$c_{02} = -8187.34$
$a_{13} = -1.33828$	$b_{03} = 443.751$	$c_{03} = 809.445$
$a_{20} = 0.0141746$	$b_{10} = -3.37282$	$c_{10} = 58.8717$
$a_{21} = 0.0205901$	$b_{11} = 35.6259$	$c_{11} = -157.626$
$a_{22} = -0.0335068$	$b_{12} = -9.35584$	$c_{12} = 75.4358$
$a_{23} = 0.983941 \cdot 10^{-2}$	$b_{13} = -1.88406$	$c_{13} = -8.79996$
$a_{30} = -0.232211 \cdot 10^{-4}$	$b_{20} = 0.0190504$	$c_{20} = -0.181846$
$a_{31} = -0.546586 \cdot 10^{-4}$	$b_{21} = -0.101348$	$c_{21} = 0.458253$
$a_{32} = 0.826651 \cdot 10^{-4}$	$b_{22} = 0.0388078$	$c_{22} = -0.22754$
$a_{33} = -0.237136 \cdot 10^{-4}$	$b_{23} = -0.129776 \cdot 10^{-4}$	$c_{23} = 0.0301332$
$a_{40} = 0.156498 \cdot 10^{-7}$	$b_{30} = -0.18162 \cdot 10^{-4}$	$c_{30} = 0.187835 \cdot 10^{-3}$
$a_{41} = 0.471533 \cdot 10^{-7}$	$b_{31} = 0.921974 \cdot 10^{-4}$	$c_{31} = -0.438936 \cdot 10^{-3}$
$a_{42} = -0.664841 \cdot 10^{-7}$	$b_{32} = -0.476565 \cdot 10^{-4}$	$c_{32} = 0.225584 \cdot 10^{-3}$
$a_{43} = 0.185212 \cdot 10^{-7}$	$b_{33} = 0.515993 \cdot 10^{-5}$	$c_{33} = -0.332753 \cdot 10^{-4}$

The a_{ij} , b_{ij} and c_{ij} are the coefficients of the polynomials and they are given in Table 2. Eqns. 5–8 describe the experimental, interpolated and extrapolated results between molalities $m = (0 \text{ to } 3.27773) \text{ mol kg}^{-1}$ with $\pm 0.011\%$ average percent, 0.125 kg m^{-3} standard and 0.084 kg m^{-3} absolute deviations. During the molality m dependence analysis of experimental results, the (p, ρ, T) properties of ethanol from Refs.^{13–15} were used.

The short empiric equation (9) can be used for the technical calculation of the (p, ρ, T) properties of ethanol solutions of LiNO_3 :

$$p = (d_1 T + d_2 m^2 T + d_3 T^2 + d_4 m T^2 + d_5 m^2 T^2 + d_6 T^3) \rho^2 + (e_1 T + e_2 m T + e_3 T^3 + e_4 m T^3) \rho^8 + f m T \rho^{12}$$

Equation (9) describe the experimental, interpolated and extrapolated results between molalities $m = (0 \text{ to } 3.27773) \text{ mol kg}^{-1}$ with $\pm 0.031\%$ average percent, 0.307 kg m^{-3} standard and 0.247 kg m^{-3} absolute deviations. The coefficients of the equation (9) $d_1, d_2, d_3, d_4, d_5, d_6, e_1, e_2, e_3, e_4$ and f are given in Table 3.

Figures 2–5 show the plots of experimental density ρ_{exp} of the $(\text{LiNO}_3 + \text{C}_2\text{H}_5\text{OH})$ versus pressure p at $m = 0.60237 \text{ mol kg}^{-1}$, at $T = 298.15 \text{ K}$ and in various molali-

ties, versus molality m at $T = 298.15 \text{ K}$ together with literature values and interpolated results at $p = 10 \text{ MPa}$, deviations of experimental density ρ_{exp} from calculated density ρ_{cal} versus pressure.

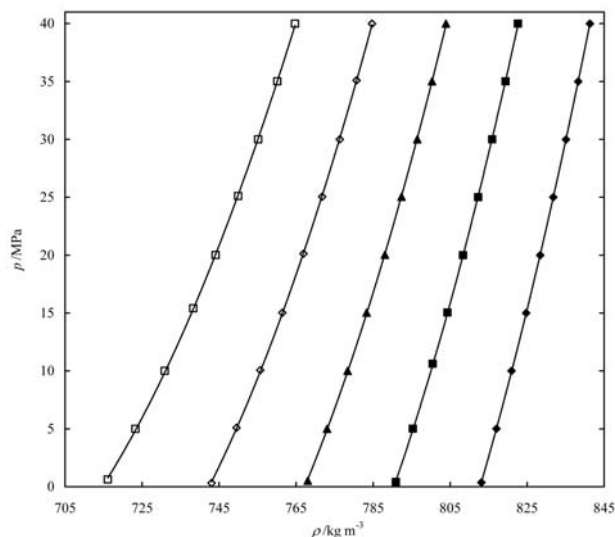


Figure 2. Plot of pressure ρ of ethanol solutions of LiNO_3 vs experimental density p at $m = 0.60237 \text{ mol kg}^{-1}$: \blacklozenge , 298.15 K; \blacksquare , 323.15 K; \blacktriangle , 348.15 K; \diamond , 373.15 K; \square , 398.15 K; ___ calculated by eqs. 5–8.

Table 3: Values of the coefficients d_i , e_i and f in Eqn. 9

d_i	e_i	f
$d_1 = -3.2550435$	$e_1 = 3.6667154436$	$f = 0.5329543$
$d_2 = 0.10916524$	$e_2 = -1.3891687$	
$d_3 = 0.0110161347$	$e_3 = -0.4077081 \cdot 10^{-5}$	
$d_4 = -0.1795944123 \cdot 10^{-3}$	$e_4 = 0.24787472 \cdot 10^{-5}$	
$d_5 = -0.18886651 \cdot 10^{-3}$		
$d_6 = -0.90607211 \cdot 10^{-5}$		

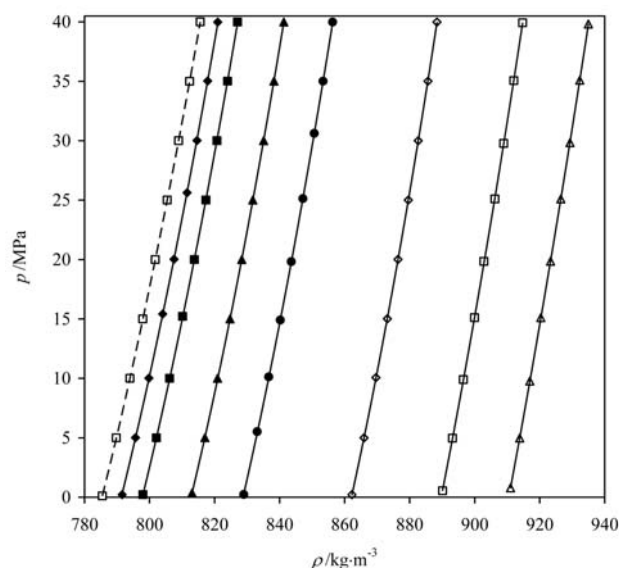


Figure 3. Plot of pressure p of ethanol solutions of LiNO_3 vs experimental density ρ at $T = 298.15$ K: \square , $m = 0$ (from Refs. [13–15]); \blacklozenge , $m = 0.12071$ mol kg^{-1} ; \blacksquare , $m = 0.26234$ mol kg^{-1} ; \blacktriangle , $m = 0.60237$ mol kg^{-1} ; \bullet , $m = 0.97956$ mol kg^{-1} ; \diamond , $m = 1.83765$ mol kg^{-1} ; \square , $m = 2.62045$ mol kg^{-1} ; Δ , $m = 3.27773$ mol kg^{-1} ; ___ calculated by eqs. 5–8.

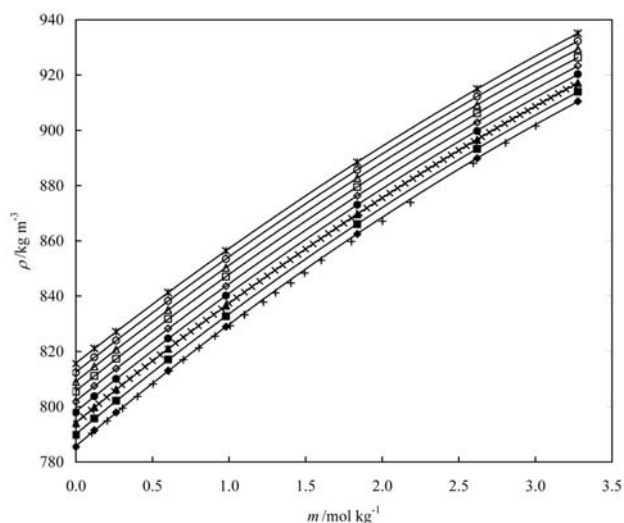


Figure 4. Plot of experimental density ρ of ethanol solutions of LiNO_3 versus molality m at $T = 298.15$ K: \blacklozenge , $p = 0.101$ MPa; \blacksquare , $p = 5$ MPa; \blacktriangle , $p = 10$ MPa; \bullet , $p = 15$ MPa; \diamond , $p = 20$ MPa; \square , $p = 25$ MPa; Δ , $p = 30$ MPa; \circ , $p = 35$ MPa; $*$, $p = 40$ MPa; $+$, ref. [8]; x , interpolated values at $p = 10$ MPa by eqs. 5–8; ___ calculated values by eqs. 5–8.

The graphical analysis of the temperature dependence of the coefficients of eqn. (5) revealed that, at $T \rightarrow T_c$, $A \rightarrow 0$. Such behavior of $A = f(T)$ may be explained by the fact that, according to Putilov,²⁰ the first term on the right-hand side of eqn. (5), $A\rho^2$, is the attractive force (attractor pressure), and the second and third terms are the repulsive

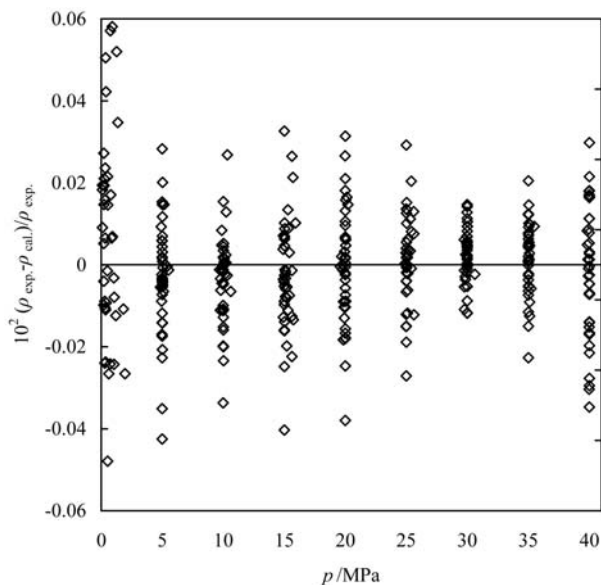


Figure 5. Plot of deviations of experimental density ρ_{exp} from the calculated by eqs. 5–8 density ρ_{cal} vs pressure p at $T = (298.15$ to $398.15)$ K and all experimental molalities.

force (repulsive pressure). As the temperature rises, the spacing between molecules increases, which contributes to a decrease in the attractive force. As the attractive force tends to zero ($A \rightarrow 0$) and molecules under the effect of the repulsive force are capable of displacement. The extent of their displacement is defined only by the density of the substance, i.e., external pressure. As a result, the aggregate state changes. Note that the form of eqn. (5) was derived from Putilov's molecular-kinetic theory.

The isothermal compressibility k/MPa^{-1} is a measure of the relative volume change of a fluid as a response to a pressure change at the constant temperature:

$$k_T = (1/\rho)(\partial p/\partial \rho)_T^{-1}, \quad (10)$$

It can be calculated from the experimental (p, ρ, T) results of ethanol solutions of LiNO_3 using eqns. (5–8) as follow:

$$k_T = 1/(2A\rho^2 + 8B\rho^8 + 12C\rho^{12}), \quad (11)$$

The calculated values of the isothermal compressibilities k $10^6/\text{MPa}^{-1}$ are given in Table 1 and for molality $m = 0.60237$ mol kg^{-1} shown in Figure 6.

The other thermal coefficient can be calculated from eqns. (5–8) is a isobaric thermal expansibility α_p/K^{-1} , which is the tendency of matter to change in volume in response to a change in temperature. When a sample is heated, its constituent particles move around more vigorously and by doing so generally maintain a greater average separation. Samples that contract with an increase in temperature are very uncommon; this effect is limited in size, and only occurs within limited temperature ranges.

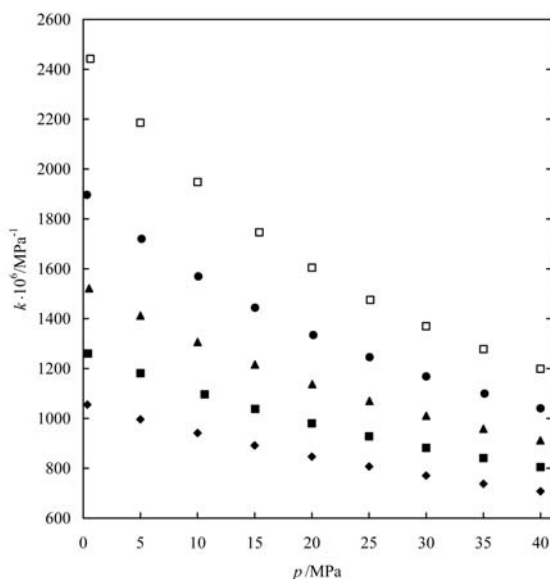


Figure 6. Plot of isothermal compressibility $k \cdot 10^6 / \text{MPa}^{-1}$ of ethanol solutions of LiNO_3 versus pressure p at $m = 0.60237 \text{ mol kg}^{-1}$ (◆, 298.15 K; ■, 323.15 K; ▲, 348.15 K; ●, 373.15 K; □, 398.15 K).

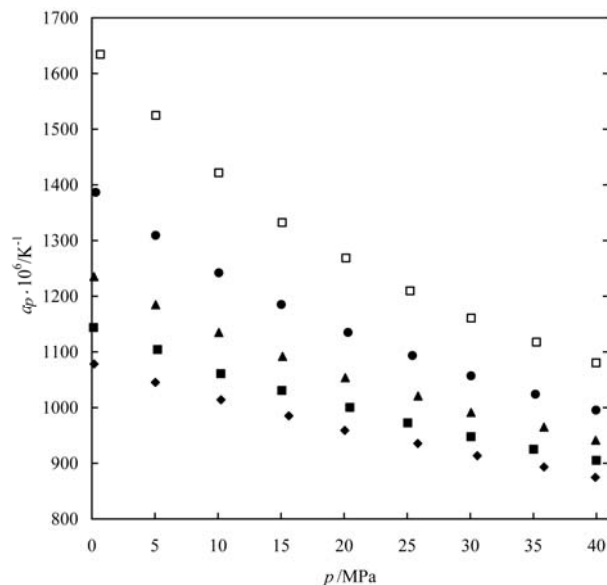


Figure 7. Plot of isobaric thermal expansibilities $\alpha_p \cdot 10^6 / \text{K}^{-1}$ of ethanol solutions of LiNO_3 vs pressure p at $m = 2.62045 \text{ mol kg}^{-1}$ (◆, 298.15 K; ■, 323.15 K; ▲, 348.15 K; ●, 373.15 K; □, 398.15 K).

The degree of expansion divided by the change in temperature is called the sample's coefficient of thermal expansion and generally varies with temperature.

$$\alpha_p = (1/\rho)(\partial p / \partial T)_p (\partial p / \partial \rho)_T^{-1}, \quad (12)$$

Isobaric thermal expansibility α_p / K^{-1} calculated from the experimental (p , ρ , T) results of ethanol solutions of LiNO_3 using the Eqns. (5–8):

$$\alpha = (A' + B' \rho^6 + C' \rho^{10}) / (2A + 8B\rho^6 + 12C\rho^{10}), \quad (13)$$

where: A' , B' , and C' are the derivatives of the A , B , and C :

$$A' = \sum_{i=1}^4 iT^{i-1} \sum_{j=0}^3 a_{ij} m^j, \quad B' = \sum_{i=1}^3 iT^{i-1} \sum_{j=0}^3 b_{ij} m^j, \quad (14)$$

$$C' = \sum_{i=1}^3 iT^{i-1} \sum_{j=0}^3 c_{ij} m^j$$

The calculated values of the isobaric thermal expansibility $\alpha_p \times 10^6 / \text{K}^{-1}$ are given in Table 1 and for molality $m = 2.62045 \text{ mol kg}^{-1}$ shown in Figure 7.

The next important parameter for the investigation is difference in specific heat capacities. Measuring the heat capacity at constant volume can be prohibitively difficult for liquids. That is, small temperature changes typically require large pressures to maintain a liquid at constant volume implying the containing vessel must be nearly rigid or at least very strong. Instead it is easier to measure the heat capacity at constant pressure and solving for the specific heat capacity at constant volume using mathematical relationships derived from basic thermodynamic laws:

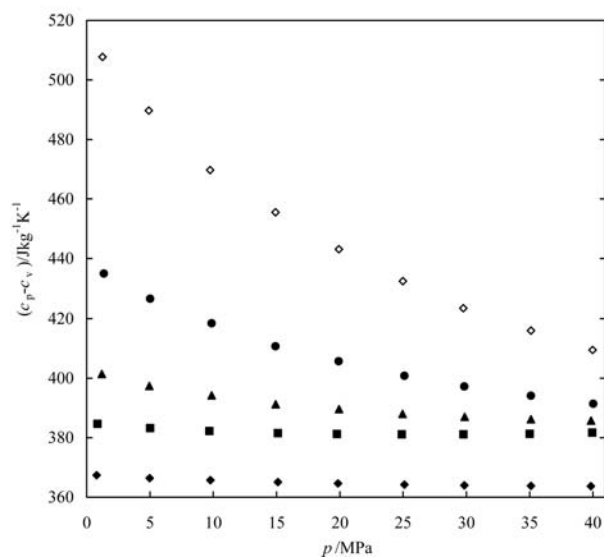


Figure 8. Plot of difference in specific isobaric and isochoric heat capacities $(c_p - c_v) / (\text{J kg}^{-1} \text{K}^{-1})$ of ethanol solutions of LiNO_3 at $m = 1.83765 \text{ mol kg}^{-1}$ versus pressure p (◆, 278.05 K; ■, 288.15 K; ▲, 298.19 K; ●, 313.18 K; ◇, 328.15 K; □, 343.18 K; △, 358.15 K; ○, 373.15 K).

$$c_p = c_v + T \frac{(\partial p / \partial T)_p^2}{\rho^2 (\partial p / \partial \rho)_T}, \quad (15)$$

where: c_p and c_v are the specific heat capacities at constant pressure and volume, respectively. Using the eqns. (5–8), we can find the following relationship:

$$c_p - c_v = \frac{\alpha_p^2 T}{\rho k_T} \quad (16)$$

The values of calculated difference in specific heat capacities are given in Table 1 and for molality $m = 1.83765 \text{ mol kg}^{-1}$ shown in Figure 8.

The apparent molar volume is the volume that

should be attributed to the LiNO_3 in the ($\text{LiNO}_3 + \text{C}_2\text{H}_5\text{OH}$) solution if one assumes that the ethanol contributes the same volume it has in its pure state. The apparent molar volume, V_ϕ , is given by

Table 4: Apparent Molar Volumes $V_\phi/(\text{cm}^3 \text{mol}^{-1})$ of the LiNO_3 in $\text{C}_2\text{H}_5\text{OH}$.

p/MPa	$m/\text{mol kg}^{-1}$						
	0.12071	0.26234	0.60237	0.97956	1.83765	2.62045	3.27773
$T = 298.15 \text{ K}$							
0.1	10.227	10.991	13.288	15.271	18.302	20.576	22.413
5	10.325	11.765	14.202	16.096	19.012	21.232	23.004
10	10.934	12.630	15.063	16.894	19.677	21.842	23.548
15	11.642	13.522	15.917	17.634	20.293	22.402	24.043
20	12.579	14.501	16.744	18.349	20.882	22.924	24.491
25	13.740	15.451	17.546	19.043	21.429	23.407	24.905
30	14.996	16.431	18.300	19.685	21.944	23.855	25.280
35	16.472	17.501	19.083	20.311	22.445	24.286	25.632
40	18.041	18.604	19.823	20.936	22.918	24.689	25.958
$T = 323.15 \text{ K}$							
0.1	11.499	11.402	12.712	14.106	16.612	18.707	20.441
5	11.793	12.405	13.881	15.244	17.607	19.614	21.271
10	12.475	13.430	15.005	16.291	18.525	20.448	22.027
15	13.390	14.532	16.084	17.263	19.364	21.199	22.704
20	14.400	15.654	17.069	18.167	20.122	21.882	23.316
25	15.907	16.860	18.047	19.040	20.847	22.520	23.885
30	17.500	18.028	18.993	19.852	21.507	23.103	24.401
35	19.052	19.222	19.885	20.609	22.130	23.646	24.873
40	20.955	20.445	20.778	21.360	22.719	24.157	25.320
$T = 348.15 \text{ K}$							
0.1	7.309	7.123	8.513	10.084	13.118	15.657	17.808
5	7.928	8.753	10.337	11.833	14.599	16.931	18.910
10	8.935	10.303	12.022	13.402	15.928	18.071	19.891
15	10.306	11.839	13.516	14.814	17.107	19.074	20.751
20	11.896	13.438	14.974	16.116	18.177	19.988	21.523
25	13.844	14.974	16.293	17.300	19.153	20.807	22.221
30	15.863	16.582	17.563	18.408	20.042	21.559	22.850
35	17.960	18.139	18.765	19.430	20.866	22.251	23.425
40	20.269	19.713	19.903	20.419	21.630	22.891	23.957
$T = 373.15 \text{ K}$							
0.24	-4.110	-3.609	-0.756	2.119	7.061	10.753	13.838
5	-2.621	-0.884	2.223	4.852	9.259	12.570	15.343
10	-0.761	1.774	4.881	7.278	11.227	14.190	16.673
15	1.733	4.349	7.304	9.448	12.941	15.601	17.818
20	4.392	6.792	9.430	11.349	14.451	16.833	18.807
25	7.227	9.191	11.401	13.060	15.800	17.927	19.679
30	10.245	11.493	13.234	14.629	17.021	18.912	20.452
35	13.301	13.777	14.940	16.069	18.131	19.801	21.149
40	16.690	15.986	16.559	17.424	19.157	20.621	21.783
$T = 398.15 \text{ K}$							
0.52	-25.038	-22.496	-15.886	-10.232	-2.080	2.961	7.035
5	-21.693	-17.582	-11.086	-6.032	1.165	5.677	9.353
10	-17.493	-12.734	-6.590	-2.142	4.153	8.160	11.450
15	-13.135	-8.381	-2.813	1.100	6.642	10.225	13.158
20	-8.737	-4.442	0.483	3.900	8.773	11.976	14.584
25	-4.102	-0.645	3.448	6.379	10.644	13.498	15.797
30	0.627	2.828	6.084	8.588	12.304	14.836	16.846
35	5.316	6.151	8.512	10.587	13.784	16.020	17.755
40	9.834	9.274	10.751	12.394	15.125	17.087	18.559

$$V_\phi = (V - n_1 V_1^0)/n_2, \quad (17)$$

where: n_1 and n_2 are the number of moles of pure ethanol and LiNO_3 , respectively; V_1^0 is the molar volume of pure ethanol. Using the density values of $(\text{LiNO}_3 + \text{C}_2\text{H}_5\text{OH})$ and pure ethanol at the high temperatures and pressures, apparent molar volumes V_ϕ of LiNO_3 in ethanol were defined by equation (18) and are listed in Table 4:

$$V_\phi = (\rho_e - \rho_s)/(m\rho_s\rho_e) + M/\rho_s, \quad (18)$$

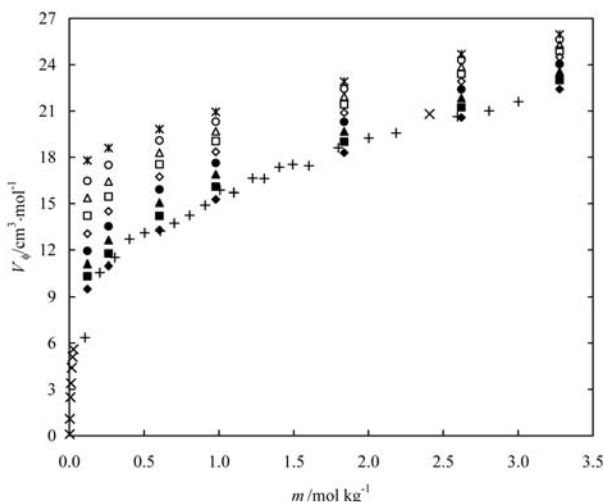


Figure 9. Plot of apparent molar volumes V_ϕ of LiNO_3 in ethanol vs m at $T = 298.15 \text{ K}$: \blacklozenge , $p = 0.1 \text{ MPa}$; \blacksquare , $p = 5 \text{ MPa}$; \blacktriangle , $p = 10 \text{ MPa}$; \bullet , $p = 15 \text{ MPa}$; \diamond , $p = 20 \text{ MPa}$; \square , $p = 25 \text{ MPa}$; Δ , $p = 30 \text{ MPa}$; \circ , $p = 35 \text{ MPa}$; $*$, $p = 40 \text{ MPa}$; \times , $p = 0.1 \text{ MPa}^7$; $+$, $p = 0.1 \text{ MPa}^8$.

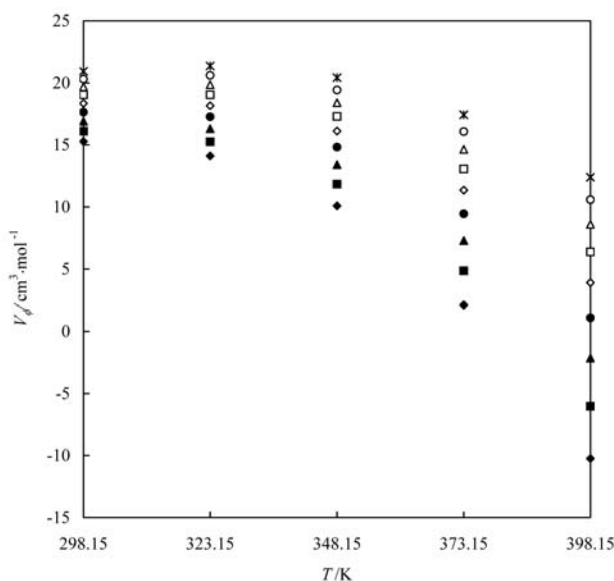


Figure 10. Plot of apparent molar volumes V_ϕ of LiNO_3 in ethanol vs temperature T at $m = 0.97956 \text{ mol kg}^{-1}$: \blacklozenge , $p = (0.24, \text{ and } 0.52) \text{ MPa}$; \blacksquare , $p = 5 \text{ MPa}$; \blacktriangle , $p = 10 \text{ MPa}$; \bullet , $p = 15 \text{ MPa}$; \diamond , $p = 20 \text{ MPa}$; \square , $p = 25 \text{ MPa}$; Δ , $p = 30 \text{ MPa}$; \circ , $p = 35 \text{ MPa}$; $*$, $p = 40 \text{ MPa}$.

where: ρ_e and ρ_s are densities of ethanol and the solutions, respectively, m is the molality and M is the molar mass of the dissolved LiNO_3 . The calculations were carried out using the density results of ethanol and $(\text{LiNO}_3 + \text{C}_2\text{H}_5\text{OH})$ at the same temperatures and pressures.

The maximum relative uncertainty²¹ δV_ϕ in the V_ϕ determination by the investigated concentrations are: $\delta V_\phi = (2.27) \%$. Figures 9 and 10 shows the plot of the apparent molar volumes V_ϕ of LiNO_3 in ethanol versus m at $T = 298.15 \text{ K}$, in various pressures together with literature results and apparent molar volumes V_ϕ of LiNO_3 in ethanol versus temperature T at $m = 0.97956 \text{ mol kg}^{-1}$.

The calculated apparent molar volume V_ϕ results were compared with 23 available literature values of [8] at $T = 298.15 \text{ K}$ and $\Delta V_\phi = 0.383 \text{ cm}^3 \text{ mol}^{-1}$ average deviation was found. The apparent molar volume results of Ref.⁸ at $T = 298.15 \text{ K}$ were added to Figure 9 for the visual comparison.

The partial molar volumes \bar{V}_i , $i = 1, 2$, are calculated from the slope of tangent $(\partial V_m / \partial x)_{p,T}$:

$$V_{\text{C}_2\text{H}_5\text{OH}} = \left[v - w \left(\frac{\partial v}{\partial w} \right)_{T,p} \right] \cdot M_{\text{C}_2\text{H}_5\text{OH}}, \quad (19)$$

$$V_{\text{LiNO}_3} = \left[v + (1 - w) \left(\frac{\partial v}{\partial w} \right)_{T,p} \right] \cdot M_{\text{LiNO}_3}$$

where: w is mass fraction of LiNO_3 and M is the relative molar masses of components of solution. The calculated values of the partial molar volumes of ethanol and LiNO_3 are presented in Table 5. Figures 11 and 12 shows the molality dependences of the partial molar volumes \bar{V}_i of ethanol and LiNO_3 at $T = 323.15 \text{ K}$ and various pressures.

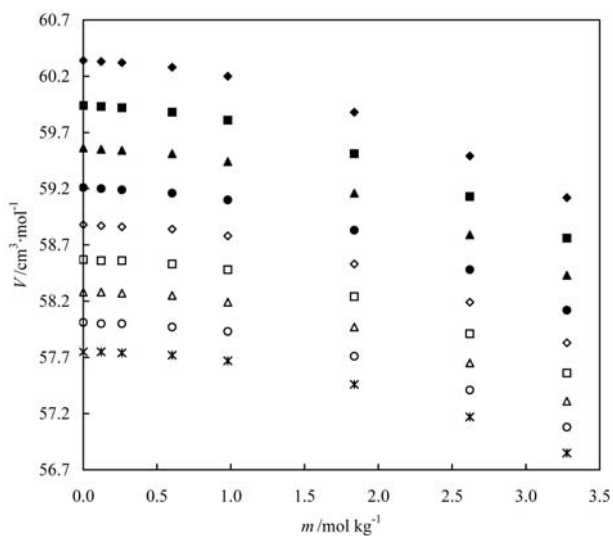


Figure 11. Partial molar volumes \bar{V}_i ($i = 1, 2$) of ethanol vs molality m at $T = 323.15 \text{ K}$ and various pressures calculated by Eqs. 19: \blacklozenge , $p = 0.101 \text{ MPa}$; \blacksquare , $p = 5 \text{ MPa}$; \blacktriangle , $p = 10 \text{ MPa}$; \bullet , $p = 15 \text{ MPa}$; \diamond , $p = 20 \text{ MPa}$; \square , $p = 25 \text{ MPa}$; Δ , $p = 30 \text{ MPa}$; \circ , $p = 35 \text{ MPa}$; $*$, $p = 40 \text{ MPa}$.

Table 5: Partial molar volumes \bar{V}_i ($i = 1, 2$) for ethanol (1) and LiNO_3 (2) derived from the density measurements.

p/MPa	$m/\text{mol kg}^{-1}$							
	0.00000	0.12071	0.26234	0.60237	0.97956	1.83765	2.62045	3.27773
$V(\text{C}_2\text{H}_5\text{OH})/\text{cm}^3 \text{mol}^{-1}$								
$T = 298.15 \text{ K}$								
0.1	58.66	58.64	58.62	58.57	58.48	58.14	57.75	57.44
5	58.33	58.31	58.30	58.25	58.16	57.83	57.46	57.14
10	58.02	58.00	57.99	57.94	57.86	57.55	57.18	56.86
15	57.72	57.71	57.70	57.66	57.58	57.27	56.92	56.60
20	57.45	57.44	57.43	57.39	57.31	57.02	56.68	56.36
25	57.19	57.18	57.17	57.13	57.06	56.78	56.45	56.14
30	56.94	56.93	56.92	56.89	56.82	56.55	56.23	55.93
35	56.71	56.70	56.69	56.66	56.59	56.33	56.03	55.73
40	56.48	56.48	56.47	56.44	56.37	56.12	55.83	55.55
$T = 323.15 \text{ K}$								
0.1	60.34	60.33	60.32	60.28	60.20	59.88	59.49	59.12
5	59.94	59.93	59.92	59.88	59.81	59.51	59.13	58.76
10	59.56	59.55	59.54	59.51	59.44	59.16	58.79	58.43
15	59.21	59.20	59.19	59.16	59.10	58.83	58.48	58.12
20	58.88	58.87	58.86	58.84	58.78	58.53	58.19	57.83
25	58.57	58.56	58.56	58.53	58.48	58.24	57.91	57.56
30	58.28	58.28	58.27	58.25	58.19	57.97	57.65	57.31
35	58.01	58.00	58.00	57.97	57.93	57.71	57.41	57.08
40	57.75	57.75	57.74	57.72	57.67	57.46	57.17	56.85
$T = 348.15 \text{ K}$								
0.1	62.29	62.28	62.27	62.22	62.12	61.74	61.24	60.76
5	61.78	61.77	61.76	61.72	61.63	61.29	60.83	60.37
10	61.31	61.30	61.29	61.25	61.18	60.87	60.44	60.00
15	60.87	60.87	60.86	60.83	60.76	60.48	60.08	59.67
20	60.47	60.47	60.46	60.43	60.37	60.11	59.75	59.36
25	60.10	60.10	60.09	60.07	60.01	59.78	59.44	59.07
30	59.76	59.76	59.75	59.73	59.68	59.46	59.14	58.80
35	59.44	59.43	59.43	59.41	59.36	59.16	58.87	58.56
40	59.13	59.13	59.12	59.10	59.06	58.88	58.61	58.32
$T = 373.15 \text{ K}$								
0.24	64.61	64.59	64.57	64.48	64.33	63.77	63.10	62.54
5	63.96	63.94	63.92	63.85	63.72	63.22	62.62	62.09
10	63.35	63.34	63.32	63.26	63.14	62.71	62.16	61.67
15	62.80	62.79	62.78	62.72	62.62	62.24	61.75	61.30
20	62.31	62.30	62.29	62.24	62.15	61.80	61.37	60.96
25	61.85	61.85	61.83	61.79	61.71	61.40	61.01	60.65
30	61.44	61.43	61.42	61.38	61.31	61.03	60.69	60.37
35	61.05	61.04	61.03	61.00	60.93	60.69	60.38	60.10
40	60.69	60.68	60.67	60.64	60.58	60.36	60.10	59.85
$T = 398.15 \text{ K}$								
0.52	67.46	67.41	67.36	67.21	66.96	66.17	65.43	65.05
5	66.61	66.58	66.53	66.40	66.19	65.50	64.82	64.41
10	65.80	65.77	65.73	65.62	65.44	64.84	64.21	63.81
15	65.08	65.06	65.03	64.93	64.78	64.24	63.68	63.29
20	64.45	64.43	64.40	64.32	64.18	63.71	63.20	62.84
25	63.88	63.86	63.84	63.77	63.64	63.22	62.77	62.44
30	63.36	63.35	63.33	63.26	63.15	62.77	62.38	62.09
35	62.89	62.88	62.86	62.80	62.70	62.36	62.02	61.78
40	62.45	62.44	62.42	62.37	62.28	61.98	61.69	61.49

p/MPa	$m/\text{mol kg}^{-1}$							
	0.00000	0.12071	0.26234	0.60237	0.97956	1.83765	2.62045	3.27773
$V(\text{LiNO}_3)/\text{cm}^3 \text{mol}^{-1}$								
$T = 298.15 \text{ K}$								
0.1	10.73	11.91	13.24	16.20	19.10	24.40	28.03	30.43
5	12.10	13.17	14.39	17.12	19.83	24.87	28.44	30.88
10	13.24	14.24	15.37	17.93	20.49	25.32	28.81	31.24
15	14.29	15.22	16.27	18.67	21.08	25.71	29.13	31.55
20	15.22	16.09	17.09	19.35	21.63	26.07	29.39	31.76
25	16.05	16.87	17.81	19.96	22.13	26.39	29.61	31.93
30	16.82	17.60	18.49	20.52	22.60	26.68	29.80	32.05
35	17.50	18.25	19.10	21.05	23.03	26.95	29.95	32.12
40	18.12	18.84	19.66	21.53	23.44	27.19	30.06	32.14
$T = 323.15 \text{ K}$								
0.1	10.42	11.31	12.32	14.66	17.08	21.91	25.67	28.46
5	12.14	12.91	13.81	15.90	18.09	22.62	26.27	29.04
10	13.59	14.28	15.09	16.98	19.01	23.27	26.80	29.53
15	14.88	15.50	16.22	17.95	19.82	23.84	27.25	29.94
20	16.03	16.59	17.24	18.81	20.55	24.35	27.65	30.28
25	17.05	17.56	18.15	19.60	21.21	24.81	28.01	30.58
30	17.95	18.41	18.95	20.29	21.79	25.23	28.33	30.85
35	18.74	19.16	19.67	20.93	22.35	25.62	28.59	31.02
40	19.47	19.86	20.33	21.50	22.84	25.97	28.84	31.21
$T = 348.15 \text{ K}$								
0.1	5.86	6.87	8.04	10.75	13.61	19.52	24.28	27.91
5	8.45	9.30	10.28	12.61	15.10	20.39	24.81	28.25
10	10.65	11.37	12.21	14.23	16.42	21.21	25.31	28.56
15	12.50	13.12	13.85	15.62	17.58	21.92	25.72	28.78
20	14.09	14.63	15.27	16.84	18.59	22.56	26.09	28.95
25	15.47	15.95	16.52	17.91	19.50	23.13	26.40	29.09
30	16.74	17.15	17.65	18.88	20.30	23.63	26.68	29.20
35	17.78	18.15	18.61	19.74	21.04	24.09	26.91	29.24
40	18.74	19.08	19.49	20.51	21.70	24.51	27.13	29.30
$T = 373.15 \text{ K}$								
0.24	-5.03	-3.21	-1.14	3.50	8.13	16.88	23.14	27.50
5	-9.0	.63	2.37	6.32	10.30	17.99	23.68	27.74
10	2.61	3.91	5.39	8.77	12.22	19.00	24.14	27.88
15	5.50	6.62	7.90	10.83	13.85	19.86	24.49	27.90
20	7.92	8.90	10.02	12.60	15.27	20.61	24.76	27.84
25	9.98	10.85	11.84	14.13	16.50	21.27	24.99	27.75
30	11.72	12.51	13.41	15.48	17.60	21.85	25.14	27.56
35	13.29	13.99	14.81	16.66	18.57	22.36	25.27	27.41
40	14.63	15.28	16.03	17.72	19.45	22.82	25.37	27.21
$T = 398.15 \text{ K}$								
0.52	-23.31	-19.74	-15.80	-7.36	.42	12.93	19.60	22.86
5	-16.46	-13.50	-10.22	-3.15	3.46	14.40	20.62	23.98
10	-10.59	-8.13	-5.39	.57	6.21	15.76	21.48	24.78
15	-6.01	-3.90	-1.55	3.58	8.47	16.90	22.11	25.23
20	-2.23	-.41	1.64	6.10	10.38	17.85	22.55	25.43
25	.86	2.47	4.27	8.23	12.02	18.65	22.85	25.44
30	3.42	4.88	6.51	10.06	13.46	19.36	23.06	25.31
35	5.65	6.97	8.45	11.66	14.71	19.96	23.19	25.10
40	7.55	8.78	10.13	13.07	15.84	20.49	23.26	24.80

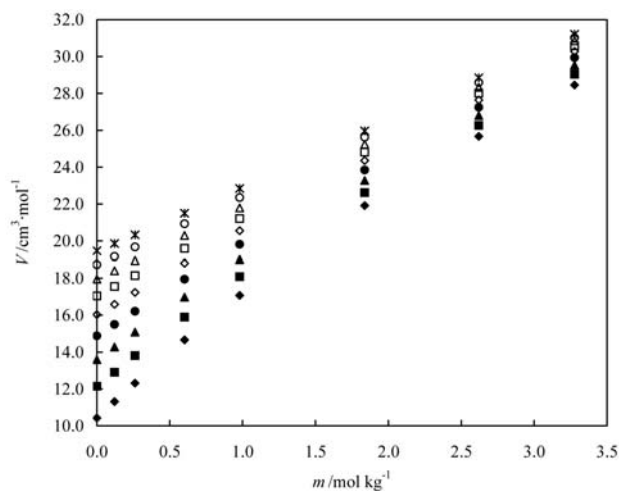


Figure 12. Partial molar volumes \bar{V}_i ($i = 1, 2$) of LiNO_3 versus molality m at $T = 323.15$ K and various pressures calculated with Eqs. 19: \blacklozenge , $p = 0.101$ MPa; \blacksquare , $p = 5$ MPa; \blacktriangle , $p = 10$ MPa; \bullet , $p = 15$ MPa, \blacklozenge , $p = 20$ MPa; \blacksquare , $p = 25$ MPa; \blacktriangle , $p = 30$ MPa; \circ , $p = 35$ MPa; $*$, $p = 40$ MPa.

4. Conclusion

For the first time, the (p, ρ, T) properties and apparent molar volumes V_ϕ of LiNO_3 in ethanol at $T = (298.15 \text{ to } 398.15)$ K and pressures up to $p = 40$ MPa are reported. An empirical correlation for the density of the investigated solutions with composition, pressure and temperature has been derived. The measured volumetric results are useful for the absorption refrigeration machines and heat pumps.

5. Acknowledgments

The authors thank Prof. Barthel for his helpful information and discussions during the many years of our research in non-aqueous electrolyte solutions field, and wish him happiness, success and health.

Dr R. Jannatliyev thanks the German Academic Exchange Service (DAAD) for the support of his research work at the Rostock University of Germany.

Povzetek

Izmerili smo gostote raztopin LiNO_3 v etanolu v širokem koncentracijskem $m = (0.12071, 0.26234, 0.60237, 0.97956, 1.83765, 2.62045, 3.27773)$ mol kg^{-1} in temperaturnem območju $T = (298.15 \text{ to } 398.15)$ K ter pri različnih vrednostih tlaka $p = (0.2 \text{ do } 40)$ MPa. Odvisnost gostot raztopin LiNO_3 v etanolu od tlaka temperature in koncentracije smo podali z empirično zvezo. Iz izmerjenih gostot smo izračunali vrednosti navidezni molskih volumnov V LiNO_3 ter parcialne molske volumne etanola ter LiNO_3 .

6. References

1. E. C. Ihmels, J. Safarov, E. Hassel, J. Gmehling, *J. Chem. Thermodyn.* **2005**, *37*, 1318–1326.
2. H. Israfilov, J. Safarov, A. Shahverdiyev, E. Hassel, *J. Chem. Eng. Data* **2008**, *53*, 388–397.
3. E. C. Ihmels, J. Safarov, *J. Mol. Liq.* **2007**, *133*, 146–151.
4. J. Barthel, R. Neueder, Chemistry Data Series, Vol. XII: Electrolyte Data Collection, Part 1a: Conductivities, Transference Numbers, Limiting Ionic Conductivities of Ethanol Solutions, DECHEMA, Frankfurt, 248 + XVIII pages, **1993**.
5. J. Barthel, R. Neueder, R. Meier, Chemistry Data Series: Vol. XII: Electrolyte Data Collection, Part 3: Viscosities of Non-aqueous Electrolyte Solutions and their Solvents I: Alcohols, DECHEMA, Frankfurt, 355 + XVII pages, **1997**.
6. J. Barthel, H. Krienke, W. Kunz, Physical Chemistry of Electrolyte Solutions, Modern Aspects, Steinkopff, Darmstadt und Springer, Berlin, **1998**, 428 p.
7. P. G. Glugla, J. H. Byon, Ch. A. Eckert, *J. Chem. Eng. Data* **1982**, *27*, 393–398.
8. O. V. Eliseeva, V. V. Golubev, E. V. Korotkova, (VINITI), Moscow, Russia, **1999**, No 12–V99.
9. Y. Marcus, G. Helter, *Chem. Rev.*, **2004**, *104*, 3406–3452.
10. S. Verevkin, J. Safarov, E. Bich, E. Hassel, A. Heintz, *J. Chem. Thermodyn.* **2006**, *38*, 611–616.
11. O. Kratky, H. Leopold, H. H. Stabinger, *Z. Angew. Physik* **1969**, *27*, 273–277.
12. W. Wagner, A. Pruß, *J. Phys. Chem. Ref. Data* **2002**, *31*, 387–535.
13. Y. Takiguchi, M. Uematsu, PVT Measurements of Liquid Ethanol in the Temperature Range from 310 to 363 K at Pressures up to 200 MPa, *J. Chem. Thermodyn.*, **1995**, *16*, 205–214.
14. Y. Takiguchi, M. Uematsu, Densities for liquid ethanol in the temperature range from 310 K to 480 K at pressures up to 200 MPa, *Int. J. Thermophys.* **1996**, *28*, 7–16.
15. H. E. Dillon, S. G. Penoncello, A Fundamental Equation for Calculation of the Thermodynamic Properties of ethanol, *Int. J. Thermophys.*, **2004**, *25*, 2 321–335.
16. R. Hilbert, pVT-Daten von Wasser und von wässrigen Natriumchlorid-Lösungen bis 873 K, 4000 Bar und 25 Gewichtsprozent NaCl, Hochschul Verlag – Freiburg, **1979**.
17. D. G. Archer, *J. Phys. Chem. Ref. Data* **1992**, *21*, 793–829.
18. E. C. Ihmels, J. Gmehling, *Ind. Eng. Chem. Res.* **2001**, *40*, 4470–4477.
19. J. T. Safarov, *J. Chem. Thermodyn.* **2003**, *35*, 1929–1937.
20. K. A. Putilov, Thermodynamics of Simplest Liquids, Issledovaniya po termodinamike (Thermodynamic Studies), Nauka, Moscow, **1973**, 105–120.
21. J. T. Safarov, G. N. Najafov, A. N. Shahverdiyev, E. Hassel, *J. Mol. Liq.* **2005**, *116*, 157–163.